Assiut Univ. J. of Botany and Microbiology ***Printed* ISSN:** *1687-4927*
47(2), p-p94-115 (2018)

ENHANCEMENT EFFECT OF IRON OXIDE NANOPARTICLES ON FERMENTATIVE BIOHYDROGEN PRODUCTION BY PURPLE NON-SULFUR BACTERIA

***Shereen M. Hamdy*[*], *Amal W. Danial*[**], *Ahmed Mohamed Abdel-Wahab*[**] *and Ahmed A.M. Shoreit*[**]**

Pediatric Hospital, Assiut University, Assiut 71516, Egypt
****Botany and Microbiology Department, Faculty of Science, Assiut University, Assiut 71516, Egypt***
Corresponding Author: ashoreit1968@yahoo.com

Received: 27/3/2018 **Accepted:** 14/8/2018 **Available Online:** 6/12/2018

In this work, the comparative impact of iron oxide nanoparticles (synthesized by orange and green tea leaf extracts) on hydrogen production by three isolates of purple non-sulfur bacteria, *Rhodobacter sphaeroides* (MG588088), *Rhodopseudomonas parapalustris* (MH094546), and *Rhodopseudomonas sp.* TUT (MG813240) was investigated. UV-vis spectra showed that the absorption band centered at a wavelength of 550 nm, which corresponds to the surface plasmon resonances of synthesized FeNPs. Fourier transformed infrared spectroscopy spectrum (FTIR) exhibited the characteristic band assigned to Fe-O. Transmission Electron microscopy (TEM) image confirmed that the average size of NPs was 32-60 nm. Nitrogenase activity was significantly stimulated by iron oxide nanoparticle and the maximum activity was recorded at 150mg/L. The hydrogen yield was significantly enhanced by FeNPs. Iron oxide nanoparticles synthesized by green tea leaves extract were more stimulatory than those extracted from orange leaves extract.

This paper is dedicated to the memory of our Prof Dr Ahmed M. Abdel-Wahab, who recently passed away.

1-INTRODUCTION

To meet the increasing demand of energy, biohydrogen production is a relevant alternative energy source in comparison with fossil fuels. Development of biotechnological systems for non-polluting fuels is a topical issue, which attracts the attention of researchers. Biological hydrogen production has several advantages (simple, non-toxic, eco-friendly and cost-effective methods) over hydrogen production by photo-electrochemical or thermochemical processes. Photosynthetic hydrogen production by microorganisms requires the use of a simple solar reactor such as a transparent closed box, with low energy requirements. Among the various hydrogen production technologies, the fermentative process for hydrogen production has more potential because it is a promising way to produce more energy from organic substrate [1]. Earlier, Shoreit [2-5] have published on the isolation and some physiological activities of purple non-sulfur bacteria in Egypt and later Danial [6,7] published on

hydrogen evolution via nitrogenase activity. Photosynthetic bacteria can produce hydrogen at the expense of solar energy and short-chain organic acids as electron donors. Phototrophic bacteria, especially *Rhodobacter capsulatus* [8-12] and *Rhodobacter sphaeroides* [8,13] are very active H_2 producers [10]. Although the major role of nitrogenase is to fix molecular nitrogen to ammonia and H_2 is produced as a by-product. It has been reported that photosynthetic bacteria can produce molecular hydrogen under suitable conditions [14-16]. Hydrogen produced during N_2-fixation by nitrogenase can be reused by uptake-hydrogenases [17]. High uptake-hydrogenase activities have been observed in cells possessing active nitrogenase; the hydrogen produced by the nitrogenase induced the activity of hydrogenase in growing cells, albeit the synthesis of hydrogenase is not closely joined to the synthesis of nitrogenase [18]. Several trace nanoparticles metals like iron, magnesium, zinc, sodium [19] and nickel [20] are important for hydrogen production due to their high surface area and small size. Iron plays vital roles in electron transport, employed in varied processes like effluent treatment and biocatalysis [21, 22]. It has also high surface reactivity and high activity capability enhancing bacterial growth and hydrogen production [20]. There are many studies conducted to check the impact of iron supplementation on photobiohydrogen production [23]. According to the previous report, supplementation of iron may oxidize the reduced ferredoxin to produce hydrogen [19]. Especially, iron is a component of ferredoxin which acts as an electron carrier in hydrogenase to produce molecular hydrogen. Many varieties of iron oxide nanoparticles like magnetite (Fe_3O_4), hematite (α-Fe_2O_3) and maghemite (γ-Fe_2O_3) have been synthesized in nature [24]. There are several physical and chemical methods that have been used to synthesize iron oxide nanoparticles (NPs). However, chemical synthesis of metal nanoparticles used different toxic chemicals that cause environmental contamination. To avoid such contamination, there is a need to develop a cost-effective, non-toxic and eco-friendly process for synthesizing iron oxide NPs. Microorganisms or plants are considered as simple, green and cost-effective to be used for synthesizing different metal nanoparticles [25]. Extraction of NPs from plants is one of the most suitable alternatives compared with those produced by physical, chemical and microbial methods. The synthesis of NPs using plant extracts is an easy and fast way compared with microbial way [26]. Green synthesis of iron nanoparticles had been accomplished using green tea [27-29], soya bean sprouts [30] and sorghum bran as a source of NP-rich extracts [31]. In continuation of the efforts, the

aromatic leaves of *Murraya koenigii* have been used for the reduction and stabilization of silver nanoparticles [32]. Philip et al. [32] and Christensen et al. [33] reported that the high concentration of soluble ingredients like carbazole, alkaloids, flavonoids and polyphenols in *M. koenigii* leaf extract had been known as accelerating the reduction and stabilization of silver nanoparticles. Mohanraj et al. [34] described a rapid technique for the synthesis of iron oxide nanoparticles using aqueous *M. koenigii* leaf extract. The objective of the present work was to study the photosynthetic H_2 production using PNS bacteria cultured in media supplemented with different concentrations of Fe-NPs synthesized using orange or tea leaf extracts. The overarching goal of our study was to improve rates of H_2 evolution.

2. MATERIALS AND METHODS

2.1 Bacterial strains and growth conditions

Bacterial strains of purple non-sulfur (PNSB) photosynthetic bacteria were isolated from wastewater and paperboard mill sludge from Assiut and Alexandria Governorate (Egypt). They were grown in RÄH medium [35] and incubated anaerobically at 30°C ± 2 at a light intensity of about 5,000 lux. Strains of PNSB were purified by the clonal selection method (serial dilution) and characterized by 16S rRNA gene sequencing using the universal primers 27 F and 1492 R.

2.2 Media composition

PNSB isolates was maintained in modified RÄH media [35]. To study the effect of iron oxide nanoparticles concentrations (50, 150 and 250 mg/L) on hydrogen production, Fe (III) chloride was omitted from the cultures, except for the control which contained 13.6 mg/L $FeCL_3$.

2.3 Synthesis and characterization of iron nanoparticles

2.3.1 Preparation of leaf extract powder-reducing agent

Twenty grams of dried leaves (orange or tea) with 1000 ml of de-ionized water were extracted at 80°C in a water bath. The extract was filtered and collected in a clean, dried beaker [36].

2.3.2 Synthesis of iron nanoparticles

Iron oxide nanoparticles were synthesized by adding green tea or orange leaves extract to 0.01 M Ferric Chloride (1:1) in a clean sterilized flask. The solution is converted to a black color, which was centrifuged and the

formed pellet was washed in water by centrifugation with deionized water to remove impurities [36].

2.3.3 Characterization of iron-NPs

2.3.3.1 UV-vis spectral analysis

The reduction of Fe^{3+} by green tea or orange leaves was monitored by UV-vis absorption spectra of the solution using (spectrophotometer thermoscientific, double beam spectrophotometer, Evolution 160, Germany) in the range of 200 nm to 1100 nm.

2.3.3.2 Transmission electron microscopy (TEM) analysis

The morphology of the Fe-NPs was investigated by TEM using JEOL-JEM-100 CXII instrument by drying a drop of the washed colloidal dispersion on to a copper grid covered with a conductive polymer.

2.3.3.3 Fourier transform infrared spectroscopy (FTIR) spectrophotometer

FTIR spectra of vacuum dried Fe-NPs were recorded as KBr pellet on Thermoscientific Nicolet 6700 FTIR spectrometer (Thermo Fisher Scientific, USA) Perkin Elmer RX1 model in the range of 4000-400cm^{-1}.

2.3.3.4 X-ray diffraction (XRD) analysis

XRD was performed using X-ray diffractometer (Model PW 1710 control unit Philips Anode Material Cu, 40 KV, 30 M.A, optics: Automatic divergence slit) with Cu Kα radiation λ=1.5405°A over a wide range of Bragg angles ($20^{\circ} \leq 2\theta \leq 90^{\circ}$). An elemental analysis of the sample was examined by energy dispersive analyses of X-rays with JED-2300 instrument.

2.4 Fermentative hydrogen production

Experiments were performed in 700-ml glass serum bottles containing 10% phosphate buffer, 10% early log phase bacterial cells, and 10% glucose made up to volume with distilled H_2O (initial pH 7± 0.2). After capping the bottle with a gastight rubber stopper and parafilm, the headspace air was displaced by nitrogen gas to generate anoxic conditions. Under aseptic conditions, bottles were stirred by magnetic stirrer as long as hydrogen is evolving. The experimental setup was maintained at $32^{\circ}C \pm 2$ and illumination provided with 200 W tungsten lamp adjusted to provide a uniform light intensity of 5000 lux. The H_2

produced was captured in a cylinder inverted in water, and connected to NaOH (2 M) solution to absorb carbon dioxide.

2.5 Nitrogenase assay

Nitrogenase activity (acetylene reduction to ethylene) was measured by gas chromatography [37-39]. The acetylene reducing activity of the growing cultures was determined at 24-h intervals throughout their growth cycle. Two ml of the headspace from each 25-ml serum bottle was withdrawn. The bottles were then injected with 2 ml acetylene (10% of the glass bottle volume) and incubated for 2 h at 30°C. Using 1ml plastic syringes, 0.5 ml of the gas mixture was withdrawn from each bottle periodically and injected into the gas chromatograph. Nitrogenase activity is expressed as nanomoles C_2H_4 produced per mg protein and the mean values of three replicates are presented.

2.6 Uptake hydrogenase assay

Uptake activity of the bidirectional hydrogenase (Hup) was assayed in a mixture containing 1 ml bacteria, 2.75 ml phosphate buffer (50 mM), 0.25 ml methylene blue (50 mM), flushed with hydrogen as conducted by Yu et al., [40] and Colbeau et al., [18]. Hydrogenenase was monitored at 574 nm (spectrophotometer thermoscientific, double beam spectrophotometer, Evolution 160, UV-VIS, Germany).

2.7 Statistical analysis

Statistical analysis of the data was conducted using ANOVA one-way test (analysis of variance) by SPSS program version 21, and Duncan values were determined at 0.05 levels.

3. RESULTS & DISCUSSION

3.1 Identification of bacterial isolates

This work has been devoted to study the hydrogen evolution capacity and the nitrogen fixing activity in three purple non sulfur bacterial strains isolated from wastewater and paperboard mill sludge from Assiut and Alexandria Governorates (Egypt). In addition, a number of trials, depending on the organism, have been attempted to enhance the magnitude of hydrogen yield. The studied purple non-sulfur bacteria were isolated and grown in RÄH medium. The isolates were identified by comparative 16S rRNA gene sequencing as *Rhodobacter sphaeroides* MG588088 and *Rhodopseudomonas*

parapalustris MH094546 (Fig 1). The third isolate (*Rhdopseudomonas sp*. TUT. MG813240) was previously identified [7].

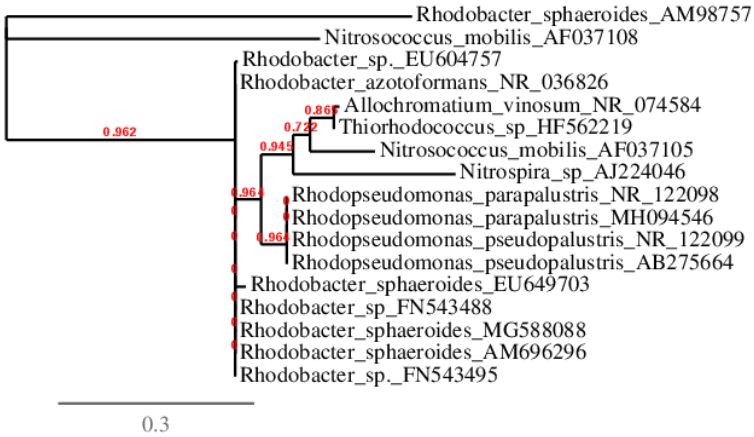

Fig 1: Phylogenetic tree on the basis of the patterns and the genetic relationship of *Rhodobacter sphaeroides* (MG 588088) and *Rhodopseudomonas parapalustris* (MH094546)

3.2 Physical characterization of the nanomaterial

3.2.1 UV-vis spectral analysis

The UV-visible absorption spectrum of the colored solution (Fig2 a, b) as a broad absorption with the absorption center at about 520-550 nm were similarly obtained by Xiaodong et al. [41] confirmed the synthesis of Fe-NPs. UV visible absorption spectrum of nano-iron sample was wide and this may be owing to different shapes and sizes of nanoparticles.

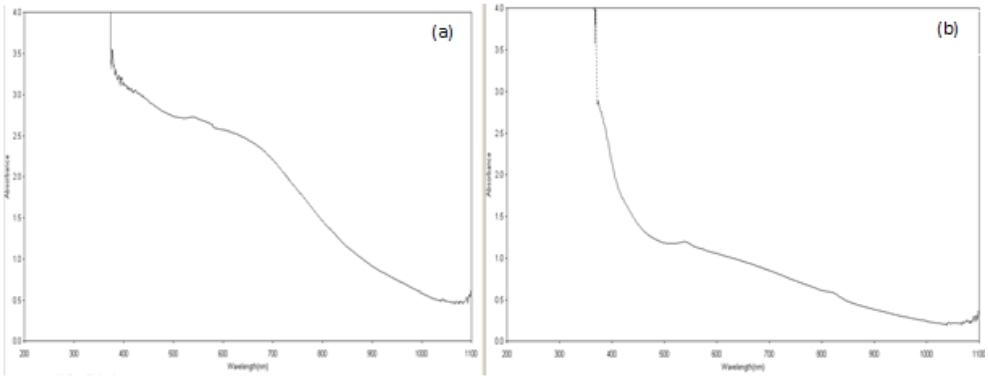

Fig. 2: UV–visible absorption spectra of iron oxide nanoparticles synthesis by reaction mixtures from orange (a) or tea (b) leaf extracts.

3.2.2 TEM images of iron nanoparticles

TEM image (Fig3 a, b) showed the morphology and size of the hydrated nanoparticles in the range of 32- 60 nm. The nanoparticles were irregularly shaped and agglomerated to each-other. The formation of varied particle sizes is also because of the agglomeration of nanoparticles throughout the sample preparation for TEM analysis.

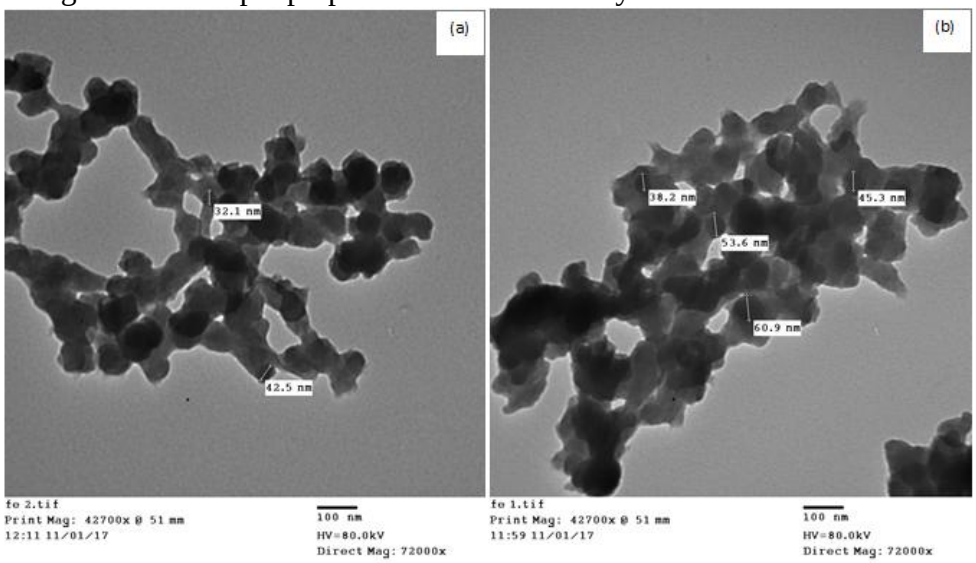

Fig. 3: TEM image of iron oxide nanoparticles at bar scale 100 nm of orange (a) or tea (b) leaf extracts.

3.2.3 FTIR spectroscopy

The FTIR spectrum of iron oxide nanoparticles (Fig4 a,b) synthesized by green tea or orange leaves extracts showed bands at 3,350, 2,923, 1,627.63, 1,365.35, 1,066.06 and 520.46 cm^{-1} and at bands 3338.62, 1629.07, 1383.34, 1266.88, 1065.51, 694.27, 418.21 ;respectively. A strong absorption band was recorded at 520.46 cm^{-1} in the case of green tea and at 418.12 in the case of orange leaves, which is typically assigned to the Fe–O bond of Fe_2O_3 as reported at earlier literature [34, 42, and 43]. The absorption bands at 3,350, 1,627.63 and 1,066.06 cm^{-1} indicated that the synthesized iron oxide nanoparticles may be surrounded by polyphenols, proteins, and amines. These findings indicate that the biomolecules present in *Camellia sinensis* and *citrus Sinensis* leave extracts may account for the reduction of Fe ions and stabilization of iron nanoparticles in an aqueous medium.

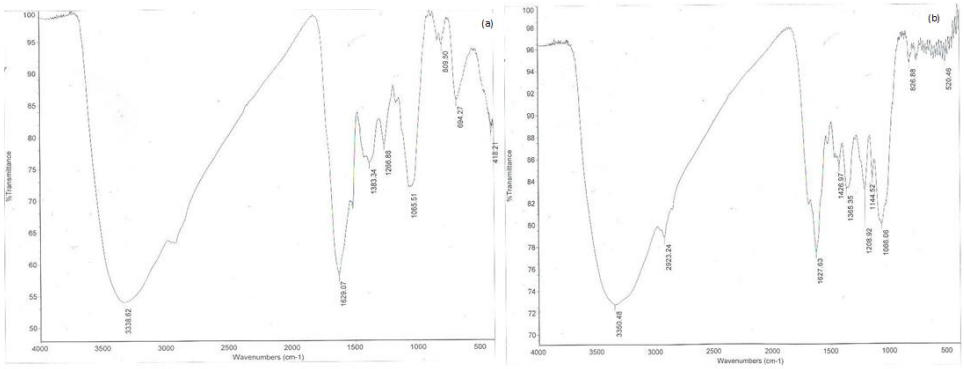

Fig 4: FTIR spectra of iron oxide nanoparticles product of orange (a) or tea (b) leaf extracts.

3.2.4 X-ray diffraction (XRD) analysis

The XRD pattern (Fig5 a, b) of the iron oxide nanoparticles synthesized by orange and green tea leaf is shown in five distinct diffraction peaks in case of green tea at 2θ values of 22.3°, 25.308°, 53.14°, 71.98°, 87.64° and eight distinct diffraction peaks in case of orange leaves at 2θ values of 25.485°, 40.0°, 41.32°, 41.86°, 45.82°, 47.62°, 52.9°, 72.16°. They matched the diffraction peaks for pure hematite (Fe_2O_3) from the reference database (JCPDS File No.19-629) according to table (1).

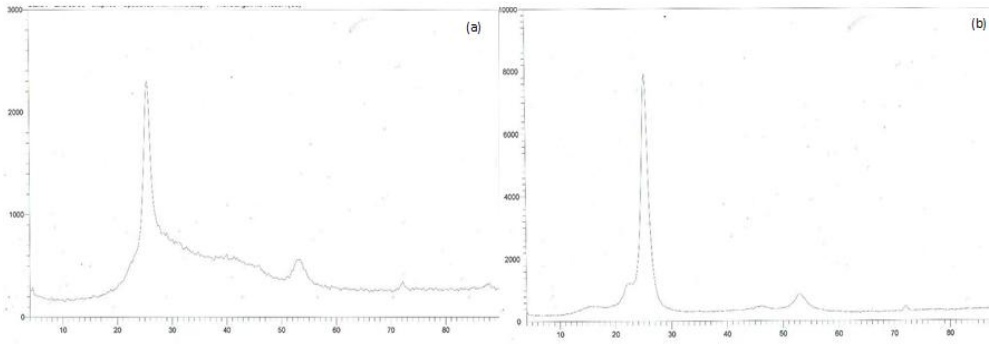

Fig 5: XRD pattern of synthesized Fe-NPs of orange (a) or tea (b) leaf extracts.

Table1: Standard XRD data of hematite and resulting samples.

Standard data		Experimental data			
Fe_2O_3		Nanparticle from orange leaves		Nanoparticle from green tea	
2θ	D	*2θ*	D	*2θ*	d
22.2489	3.992320	-	-	22.3	3.987
26.7983	3.323990	25.485	3.495	25.308	3.519
40.2029	2.241250	40.0	2.254	-	-
41.5507	2.171610	41.32	2.185	-	-
42.1082	2.144140	41.86	2.158	-	-
45.8476	1.977580	45.82	1.98	-	-
47.3012	1.920140	47.62	1.91	-	-
52.9904	1.726610	52.9	1.731	53.14	1.724
71.7720	1.314080	72.16	1.309	71.98	1.312
87.7267	1.1.111610	-	-	87.64	1.113

3.3 Effect of Iron Oxide Nanoparticles on nitrogenase, hydrogenase and cumulative hydrogen production.

The concentrations of iron oxide nanoparticles were applied in the range from 0 to 250 mg/L to evaluate the enhancement effect of nitrogenase, hydrogenase and hydrogen production.

The hydrogen evolution and % substrate conversion efficiency (SCE) at different concentrations of iron oxide nanoparticles are shown in table (2). The maximum hydrogen yield formed was 3400 and 3600 ml H_2/L correspondingly to 150 mg/L NPs synthesized from orange and green tea leaves; respectively (Fig 6) in case of *Rhodobacter sphaeroides*.

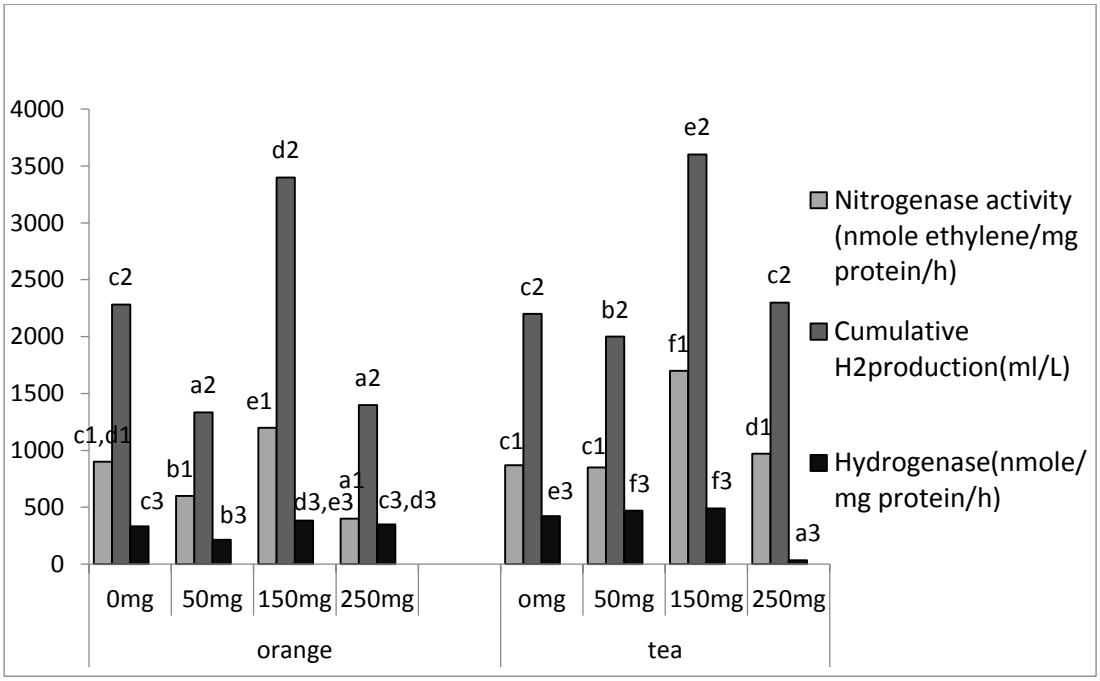

Fig 6: Effect of iron oxide nanoparticle concentrations synthesized by orange and green tea leaves extract on nitrogenase, hydrogenase activity and cumulative hydrogen production by *Rhodobacter sphaeroides* (MG588088). The ANOVA test was carried out by using SPSS 21 comparisons among means ± SE standard error (n=3), different letters show significance at p = 0.05 level based on Duncan's multiple range test.

Nitrogenase and hydrogenase activities were also significantly stimulated by iron oxide NPs, and the maximum activity was also recorded at 150 mg/L NPs. The results (Fig 6) indicated that iron oxide nanoparticles synthesized by orange and green tea leaves extracts enhanced the activities of these enzymes to 1200, 384 and 1700, 491 nmol/mg protein/ h; respectively.

Figure (7) clearly shows that the addition of iron nanoparticles to *Rhodopseudomonas parapalustris* isolate (MH094546) significantly accelerated H_2 production with a parallel increase in nitrogenase activity, which increased to 1.7 and 1.6 folds with supplementation of NPs synthesized by orange and green tea leaves extract; respectively.

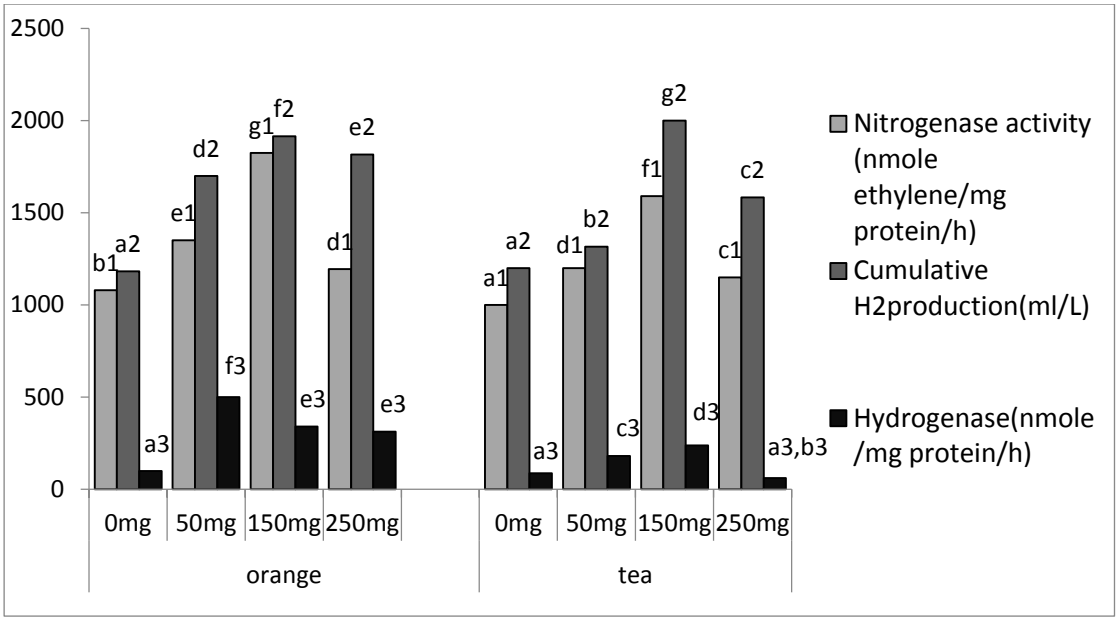

Fig 7: Effect of iron oxide nanoparticle concentrations synthesized by orange and green tea leaves extract on nitrogenase, hydrogenase activity and cumulative hydrogen production by *Rhodopseudomonas parapalustris* (MH094546). The ANOVA test was carried out by using SPSS 21 comparisons among means ± SE standard error (n=3), different letters show significance at p = 0.05 level based on Duncan's multiple range test.

The data in fig (8) showed that the hydrogen-producing bacteria *Rhdopseudomonas sp*. TUT MG813240 responded significantly to the addition of nanoparticles. The hydrogen evolution and percentage of hydrogen increased significantly compared with the control cultures. The maximum yield was 1620 and 2100 ml with the addition of 150 mg/L NPs synthesized using orange and green tea leaves extract; respectively.

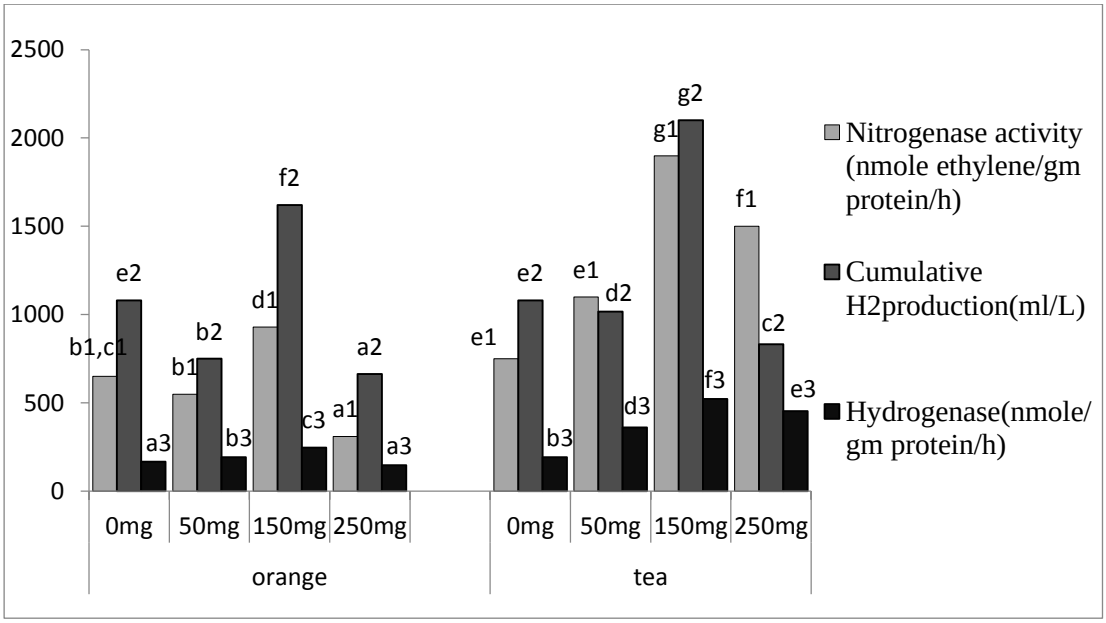

Fig 8: Effect of iron oxide nanoparticle concentrations synthesized using orange and green tea leaves extract on nitrogenase, hydrogenase activity and cumulative hydrogen production by *Rhdopseudomonas sp* TUT MG813240. The ANOVA test was carried out by using SPSS 21 comparisons among means ± SE standard error (n=3), different letters show significance at p = 0.05 level based on Duncan's multiple range test.

The results indicated that the enhancement of hydrogen production was strongly dependent on the concentration of iron nanoparticles, and 150mg/L was the optimal concentration to catalyze the highest biohydrogen level in our studied strains.

The hydrogen production rate was significantly enhanced by the supplementation of FeNPs with increasing concentration from 100 to 150 mg/L and further it was not favourable to improve the H_2 production rate at concentration over 150 mg/L. This may be due to the fact that the high concentration of FeNPs could inhibit the activity of PNSB. The high concentration of hematite nanoparticles (150 mg/l) promoted the start-up of hydrogen production rate, but the excess soluble hematite nanoparticles was harmful to the microorganisms, and resulted in the decrease of hydrogen production rate.

The uptake hydrogenase activity (hup) was also enhanced by the addition of iron nanoparticles in the original medium (Fig 6, 7, 8) for the three studied bacteria. Maximum activity of hup was recorded in *Rhodobacter sphaeroides* (MG588088) with 150 mg/L nanoparticle from both orange and green tea leaves extract, as 384 and 491 nmol/mg

protein/h, respectively. In the case of *Rhodopseudomonas parapalustris* (MH094546), maximum activity was 340 and 238 nmol/mg protein/h while *Rhdopseudomonas sp.* TUT (MG813240) exhibited maximum activity for hydrogenase as 247 and 522 nmol/mg protein/h; respectively.
Fe essentially forms the metallic part of nitrogenase as well as that of hydrogenase structure and more over also contributes in electron transfer chain (ETC) in the form of electron carriers like ferredoxin and cytochromes, so the ferredoxin activity could also be increased by the supplementation of FeNPs throughout the fermentation method [34]. According to the literature, the supplementation of FeNPs improved the nitrogenase activity that led to enhance the fermentative hydrogen production [44]. The most active strain in our study was *Rhodobacter sphaeroides* (MG588088) in both nitrogenase activity and hydrogen production yield. Also, nanoparticles synthesized by green tea leaf extract gave the highest rate of hydrogen evolution compared with NPs extracted from orange leaves extract in all studied bacteria.
The data in table (2) showed that the hydrogen-producing bacteria responded a quickly to the addition of nanoparticles. The yield and percentage of hydrogen increased significantly compared with the control. The maximum yield by *Rhodobacter sphaeroides* (2.2 mol H_2/mol glucose) and (4 mol H_2/mol glucose) obtained in presence of 150 mg/L iron nanoparticles from orange and green tea; respectively. In the case of *Rhodopseudomonas parapalustris* (MH094546), the maximum yield was 1.7 and 1.34 mol H_2/mol glucose and in the case of *Rhdopseudomonas sp.* TUT the maximum yield was 1.04 and 1.4 mol H_2/mol glucose.

Table 2: The fermentation profiles of hydrogen production on glucose using PNS bacteria added with different concentrations of iron nanoparticles (0-250 mg/l):

Source of NPS	**Treatment**	***Rhodobacter sphaeroides* MG588088**			***Rhodopseudomonas parapalustris* (MH094546)**			***Rhdopseudomonas TUT*. MG813240**		
		Hydrogen yield(L/L)	Mole H_2/mole glucose	H_2 efficiency (L/gm)	Hydrogen yield(L/L)	Mole H_2/mole glucose	H_2 efficiency (L/gm)	Hydrogen yield(L/L)	Mole H_2/mole glucose	H_2 efficiency (L/gm)
	Cont	2.283	1.28	0.16	1.183	0.64	0.08	1.083	0.71	0.09
Orange	50mg	1.333	0.73	0.09	1.7	1.04	0.14	0.75	0.47	0.06
	150mg	3.4	2.2	0.28	1.967	1.7	0.21	1.633	1.04	0.14

	250mg	1.4	1.05	0.14	1.816	1.02	0.13	0.666	0.38	0.05
Tea	50mg	2	1.8	0.22	1.316	0.75	0.09	1.016	0.75	0.09
	150mg	3.6	4	0.51	2	1.34	0.17	2.1	1.4	0.184
	250mg	2.3	1.4	0.17	1.583	1	0.12	0.833	0.54	0.06

From a previous study, Mohanraj et al. [34] confirmed that the hydrogen yield in control experiments was obtained as 1.74±0.08 mol H_2/mol glucose whereas the highest hydrogen yield in FeNPs supplemented experiment was achieved as 2.33±0.09 mol H_2/mol glucose at 175 mg/L of FeNPs by *Clostridium acetobutylicum* NCIM 2337. Dolly et al. [45] reported that significant enhancement in light dependent fermentative hydrogen production using iron oxide nanoparticles was 1.2 fold compared with control culture; these results were in agreement with our ones. In another work, Engliman et al. [46] recorded that the hydrogen production by anaerobic mixed bacteria in thermophilic condition using iron (II) oxide nanoparticles increasing to 34.38% higher than the control test.

Tables (3, 4) showed a comparative study of hydrogen evolution by different cultures and different nanoparticles compared with this study.

In this work, the hydrogen efficiency at iron nanoparticles (from orange) was 75, 162 and 51 %, that are much higher than the values obtained from control culture of *R. sphaeroides* (MG588088), *Rhodopseudomonas parapalustris* (MH094546) and *Rhdopseudomonas sp.* TUT (MG813240); respectively. The maximal conversion efficiency of hydrogen production were 218, 100 and 104% at 150 mg/L iron nanoparticles from tea leaves extract for previous three isolates; respectively.

Green tea, as a reducer for the synthesis of iron oxide nanoparticles, contains a high quantity of polyphenols and other organic groups [36]. The polyphenols consist of flavonoids and catechins. The catechins primarily the Epigallocatechin Gallate (EGCG) are the active catechin that takes part in the reduction process that can reduce the Fe^{3+} to Fe^{0} [36].

Table 3: Comparison of hydrogen production by different purple non-sulfur bacteria using different substrates:

Microorganism	**H_2max (mL H_2/L)**	**Substrate**	**Reference**
Rhodobacter sphaeroides	1190	Malate	[47]

KD131			
Rhodobacter sphaeroides NMBL-01	2275	Malate	[48]
Rhodobacter sphaeroides RV	284	Malate	[49]
Rhodobacter sphaeroides ZX-5	3157	Malate	[50]
Rhodobacter sphaeroides O.U.001	650	Malate	[51]
Rhodobacter sp. KKU-PS1	1339	Malate	[52]
Rhosopseudomonas sp TUT (Rh1, Rh2 and Rh3)	900, 700 and 700	Orange peel	[6]
Rhodobacter sp	700	Orange peel	[6]
Rhodobacter capsulatus-PK	372	wheat straw	[53]
Rhodobacter sphaeroides	400	Waste barley	[54]
Rhodobacter sphaeroides NRRL B-1727 *Rhodobacter sphaeroides* DSMZ-158 *Rhodobacter sphaeroides* RV	1.23 mol H_2 /mol glucose	Wheat powder	[55]
Rhosopseudomonas sp (Rh1, Rh2)	1955 and 1400	Lactate	[7]

Table 4: The effect of different nanoparticles on fermentative hydrogen production

Inoculum	**Substrate**	**Nanoparticle**	**Concentration of nanoparticle (mg/L)**		**Hydrogen yield**	**Reference**
			Studied range	**Optimal**		
***Enterobacter cloacae* DH-89**	Glucose	FeNPs	25-200	100	0.95 (mol H_2/mol Glucose)	[56]
Cracked cereals	Sucrose	Hematite	0-1600	200	1.6 (mol H_2/mol glucose)	[57]
Anaerobic granular sludge	Starch	Iron and nickel NPs	0-50	37.5	89 mL/g VS	[58]
Anaerobic granular sludge	Glucose	Iron and nickel	0.5-100	50	1.43 (iron) 1.88 (nickel) (mol H_2/mol glucose)	[59]
Anaerobic granular sludge	Starch	Maghemite	0-25	25	2.23 (mol H_2/mol glucose)	[60]
***Clostredium acetobutylicum* NCIM 2337**	Glucose	Iron nanoparticle	50-250	175	2.33 (mol H_2/mol glucose)	[36]
Anaerobic sludge	Glucose	Nickel nanoparticle	10-50	20	3000 mL H_2/L	[61]

Anaerobic sludge	Glucose and starch	Iron and nickel oxide	0-500	50	1.92 (mol H_2/mol glucose)	[46]
***Rhodobacter sphaeroides* NMBL-02 and Escherichia coli NMBL-04**	Malate	Fe-nanoparticle	1-700	300	1870 mL H_2/L	[45]
***Rhodobacter sphaeroides* MG 588088**	Glucose	Fe_2O_3 NPs	0-250	150	4 (mol H_2/mol glucose)	This study
***Rhodopseudomonase sp* TUT MG813240**	Glucose	Fe_2O_3 NPs	0-250	150	1.4(mol H_2/mol glucose)	This study
***Rhodopseudomonas parapalustris* (MH094546)**	Glucose	Fe_2O_3 NPs	0-250	150	1.7(mol H_2/mol glucose)	This study

4. CONCLUSION

Photosynthetic bacteria are favorable candidates for biological hydrogen production because of their high conversion efficiency and versatility in the substrates they can utilize. From the results discussed above, green synthesis of nanoparticles is a promising approach for enhancing hydrogen production using three strains of purple non-sulfur bacteria. The supplementation with Fe NPs enhanced the biohydrogen production, in a concentration dependent manner. Two enzymes are especially critical for hydrogen production; nitrogenase produces hydrogen and uptake hydrogenase consumes hydrogen.

REFERENCES

[1] Wang, A.; Ren, N.; Shi, Y. & Lee, D. J. 2008. Bioaugmented hydrogen production from microcrystalline cellulose using co-culture - *Clostridium acetobutylicum* X9 and Ethanoigenens harbinense 49. International Journal of Hydrogen Energy, 33,912–917.

[2] A.A.M. Shoreit; M.H. Abd-Alla and M.S.A. Shabeb. 1992. Acetylene reduction by Rhodospirillaceae from the Aswan High Dam Lake .World Journal of Microbiology and Biotechnology, 8, 151-154.

[3] Shabeb, M. S. A. and Shoreit, A. A. M. 2006. Biosynthesis of an expected thermoplastic polythioesters *Rhodopseudomonas palustris* ASEC 47,12th .International Symposium on phototrophic prokaryotes.

[4] Shabeb, M. S. A.; Younis, M. and Shoreit, A. A. M. 2006. Isolation and Identification of Purple non-sulfur bacteria (Rhodosirillaceae) from River Nile Aswan-Egypt, New Egyptian J Microbio, 13:.176-187.

[5] Shoreit, A.A.M; E.K.dy IA and Sayed, W.F. 1994. Isolation and

identification of purple nonsulfur bacteria of mangal and non-mangal vegetation of Red Sea coast. Egypt. Limnologica, 24(2): 177-183.

[6] Danial, A. W. and Abdel-Basset, R. 2015. Orange peel inhibited hup and enhanced hydrogen evolution in some purple non-sulfur bacteria. International journal of hydrogen energy, 40 941-947.

[7] Danial, A. W.; Abdel Wahab, A. M.; Arafat, H. H. and Abdel-Basset, R. 2017. Bioenergetics of lactate vs. acetate outside TCA enhanced the hydrogen evolution levels in two newly isolated strains of the photosynthetic bacterium *Rhodopseudomonas* Z. Naturforsch ,aop.

[8] Weaver, P.F; Wall, J.D and Gest, H. 1975. Characterization of *Rhodopseudomonas capsulata.* Arch. Microbiol, 105: 207±216.

[9] Tsygankov, A.A. and Gogotov, I.N. 1982. The activities of nitrogenase and hydrogenase of *Rhodopseudomonas capsulata* during its growth under the conditions of nitrogen fixation depending on temperature and pH. Mikrobiologiia, 51: 396±401.

[10] Yakunin, A.F.; Tsygankov, A.A. and Gogotov, I.N. 1985. Ratio of two forms of nitrogenase and switch-off effect in *Rhodobacter capsulatus* grown under conditions of ammonium limitation. Dokl Akad Nauk SSSR, 281: 482±485.

[11] Steinborn, B. and Oelze, J. 1989. Nitrogenase and photosynthetic activities of chemostat cultures of *Rhodobacter capsulatus* 37b4 grown under different illuminations. Arch Microbiol, 152: 100±104.

[12] Tsygankov, A.A.; Laurinavichene, T.V. 1996. Influence of the degree and mode of light limitation on growth characteristics of the *Rhodobacter capsulatus* continuous cultures. Biotechnol Bioeng, 51: 605±612.

[13] Laurinavichene T.V.; Vasyleva L.G.; Tsygankov, A.A. and Gogotov, I.N. 1988. The purple nonsulfur bacterium *Rhodobacter sphaeroides* isolated from the rice ®eld soil of South Vietnam. Mikrobiologiia, 57: 810±815.

[14] Bowien, B.; Schlegel, H.G. 1981. Physiology and Biochemistry of Aerobic Hydrogen-Oxidizing Bacteria. Annual Review of Microbiology.

[15] Das, D. and Nejat, V. T. 2001. Hydrogen production by biological processes: a survey of literature. Int J Hydrogen Energy, 26:13–28.

[16] Kontur, W. S.; Ziegelhoffer, E. C.; Spero, M. A.; Imam, S.; Noguera ,D. R. and Donohue, T. J. 2011.Pathways Involved in Reductant Distribution during Photobiological H_2 Production by *Rhodobacter sphaeroides* . Appl Environ Microbiol, 77(20): 7425-7429.

[17] Vignais, P.M.; Billoud, B. 2007. Occurrence, classification, and biological function of hydrogenases: an overview Chem Rev, 107:4206–4272.

[18] Colbeau, A.; Kelley, B.C.; Vignais, P.M. 1980. Hydrogenase activity in *Rhodopseudomonas capsulata*: relationship with nitrogenase activity. J Bacteriol, 144:141–148.

[19] Chong, M. L.; Sabaratnam, V.; Shirai, Y. & Hassan, M. A. 2009. Biohydrogen production from biomass and industrial waste by dark fermentation.International Journal of Hydrogen Energy, 34, 277–3287.

[20] Liu, B. F.; Ren, N. Q.; Ding, J.; Xie, G. J. & Guo, W. Q. 2009. The effect of Ni^{2+}, Fe^{2+} and Mg^{2+} concentration on photo-hydrogen production by *Rhodopseudomonas faecalis* RLD-53.International Journal of Hydrogen Energy, 34,721–726.

[21] Matei, E.; Predescu, A.; Vasile, E. & Predescu, A. 2011. Properties of magnetic iron oxides used as materials for wastewater treatment. Journal of Physics: Conference Series, 304,012022.

[22] Safarikova, M.; Maderova, Z. & Safarik, I. 2009. Ferrofluid modified Saccharomyces cerevisiae cells for biocatalysis. Food Research International, 42,521–524.

[23] Eroglu, E.; Gunduz, U.; Yucel, M. and Eroglu, I. 2011. Effect of iron and molybdenum addition on photo-fermentative hydrogen production from olive mill wastewater. Int J Hydrogen Energy, 36(10):5895-903.

[24] Teja, A. S. & Koh, P. Y. 2009. Synthesis, properties, and applications of magnetic iron oxide Nanoparticles. Progress in Crystal Growth and Characterization of Materials,55, 22–45.

[25] Narayanan, K. B. & Sakthivel, N. 2010. Biological synthesis of metal nanoparticles by Microbes.Advance in Colloid and Interface Science, 156,1–13.

[26] Mohamed Abdul-Aziz Elblbesy ; Adel Kamel Madbouly and Thamer Abed-Alhaleem Hamdan.2014. Bio-synthesis of magnetite nanoparticles by bacteria. American Journal of Nano Research and Application, 2(5): 98-103.

[27] Shahwan, T.; Sirriah, S. A.; Nairat, M.; Boyaci, E.; Eroglu, A. E.; Scott, T. B. & Hallam, K. R. 2011. Green synthesis of iron nanoparticles and their application as a Fenton-like catalyst for the degradation of aqueous cationic and anionic dyes.Chemical Engineering Journal, 172,258–266.

[28] Hoag, G. E.; Collins, J. B.; Holcomb, J. L.; Hoag, J. R.; Nadagouda, M. N. & Varma, R. S. J. 2009. Degradation of bromothymol blue by greener nanoscale

zero-valent iron synthesized using tea polyphenols.Journal of Material Chemistry, 19, 8671–8677.

[29] Nadagouda, M. N.; Castle, A. B.; Murdock, R. C.; Hussain, S. M. & Varma, R. S. 2010. In vitro biocompatibility of nanoscale zerovalent iron particles (NZVI) synthesized using tea polyphenols.Green Chemistry, 12,114–122.

[30] Cai, Y.; Shen, Y.; Xie, A.; Li, S. & Wanga, X. 2010. Green synthesis of soya bean sprouts-mediated superamegnetic Fe_3O_4 nanoparticles. Journal of Magnetism and Magnetic Materials, 322, 2938–2943.

[31] Njagi, E. C.; Huang, H.; Stafford, L.; Genuino, H.; Galindo, H. M.; Collins, J. B.; Hoag, G. E. & Suib, S. L. 2011. Biosynthesis of iron and silver nanoparticles at room temperature using aqueous sorghum bran extracts. Langmuir, 27,264–271.

[32] Philip,D.; Unni,C.; Aromal,S.A.& Vidhu,V.K . 2011. Murraya koeningii leaf assisted rapid green synthesis of silver and gold nanoparticles. Spectrochimica Acta Part A: Molecular and Biomolecular Spectroscopy 78,899 –904.

[33] Christensen, L.; Vivekanandhan, S.; Misra, M. & Mohanty, A. K. 2011. Biosynthesis of silver nanoparticles using Murraya koenigii (curry leaf): an investigation on the effect of broth concentration in reduction mechanism and particle size.Advances Material Letters, 2,429 –434.

[34] Mohanraj, S.; Kodhaiyolii, S.; Rengasamy, M. & Pugalenthi,V. 2014. Green Synthesized Iron Oxide Nanoparticles Effect on Fermentative Hydrogen Production by *Clostridium acetobutylicum*. Appl Biochem Biotechnol ,173:318–331.

[35] Drews, G. Mikrobiolosches praktikum. 1983. vol. 186. Berlin, Heidelberg, New York: Springer-Verlag.

[36] Gottimukkala, K.S.V. 2017. Green Synthesis of Iron Nanoparticles Using Green Tea leaves Extract. J Nanomedicine Biotherapeutic Discov, 7: 151. doi: 10.4172/2155-983X.1000151.

[37] Hardy, R. W. F. and Knight, E .J. 1967. ATP dependent reduction of azide and HCH by N2-fixing enzymes of *Azotobacter vinelandii* and Clostridium pastorium. Biochem. Biophys. Acta ,139: 60-90.

[38] Hardy, R .W.F; Burns, R. C. and Holsten, R .D. 1973. Applications of the acetylene-ethylene assay for measurement of nitrogen fixation. Soil Biol. Blochem, 5:47-81.

[39] Hardy, R. W. F; Holsten, R.D; Jackson, E. K. and Burns, R. C.1968. The acetylene-reduction assay for N_2 fixation: Laboratory and field evaluation. Plant Physiol, 43: 1185–1207.

[40] Yu, R.S; Harmon, S.R. and Blank, F. 1969. J Invest Dermat, 53:166.

[41] Xiaodong Li; Zhi Wang; Zemin Zhang; Lulu Chen; Jianli Cheng; Wei Ni; Bin Wang & Erqing Xie. 2015. Light illuminated a αFe_2O_3/Pt Nanoparticles as Water Activation Agent for Photoelectrochemical Water Splitting. SCIENTIFIC REPORTS, 5: 9130.DOI: 10.1038/srep09130.

[42] Togashi, T.; Naka, T.; Asahina, S.; Sato, K.; Takami, S. & Adschiri ,T. 2011.Surfactant-assisted one-pot synthesis of super magnetic magnetite nanoparticle clusters tunable cluster size and magnetic field sensitivity. Dalton Transactions, 40, 1073–1078.

[43] Biswas, S.; Belfield, K. D.; Das, R. K.; Ghosh, S. & Hebard,A. F. 2012. Superparamagnetic nanocomposites template with pyrazole-containing diblock copolymers. Polymers, 4, 1211–1225.

[44] Wang, J. & Wan, W. 2008. Effect of Fe^{2+} concentration on Fermentative hydrogen production by mixed cultures. International Journal of Hydrogen Energy 33, 1215–1220.

[45] Suman Dolly; Anjana Pandey; Bishnu Kumar Pandey and Ram Gopal. 2015. Process parameter optimization and enhancement of photo-biohydrogen production by mixed culture of *Rhodobacter sphaeroides* NMBL-02 and *Escherichia coli* NMBL-04 using Fe-nanoparticle. international journal of hydrogen energy, 1-11.

[46] Engleman,N.S.; Peer Mohamed Abdul; Shu-Yii, W.u and Jamaliah Md Jahim. 2017. Influence of iron (II) oxide nanoparticle on biohydrogen production in thermophilic mixed Fermentation International journal of hydrogen energy, 1-12.

[47] Kim, M.S.; Kim, D.H. and Cha, J. 2012. Culture conditions affecting H_2 production by phototrophic bacterium *Rhodobacter sphaeroides* KD131. Int J Hydrog Energy, 37:14055 – 61. http://dx.doi.org/10.1016/j.ijhydene.2012.06.085.

[48] Pandey, A.; Srivastava, N. and Sinha, P. 2012. Optimization of hydrogen production by *Rhodobacter sphaeroides* NMBL-01. Biomass Bioenergy, 37:251–6. http://dx.doi.org/10.1016/j.biombioe.2011.12.005.

[49] Han, H.; Liu, B.; Yang, H. and Shen, J. 2012. Effect of carbon sources on the photobiological production of hydrogen using *Rhodobacter sphaeroides* RV.

Int J Hydrog Energy, 37:12167–74. http://dx.doi.org/10.1016/j.ijhydene.2012.03.134.

[50] Tao, Y.; He, Y.; Wu, Y.; Liu, F.; Li ,X. and Zong ,W.2008. Characteristics of a new photosynthetic bacterial strain for hydrogen production and its application in wastewater treatment. Int J Hydrog Energy, 33:963 – 73.

http://dx.doi.org/10.1016/j.ijhydene.2007.11.021.

[51] Basak. N. and Das, D. 2009. Photo fermentative hydrogen production using purple non-sulfur bacteria *Rhodobacter sphaeroides* O.U.001 in an annular photobioreactor: A case study. Biomass Bioenergy, 33:911 – 9.

http://dx.doi.org/10.1016/j.biombioe.2009.02.007.

[52] Thitirut Assawamongkholsiri and Alissara Reungsang. 2015. Photo-fermentational hydrogen production of *Rhodobacter sp*. KKU-PS1 isolated from an UASB reactor. Electronic Journal of Biotechnology, 18 221–230.

[53] Saima Shahzad Mirza; Javed Iqbal Qazi; Quanbao Zhao and Shulin Chen. 2013. Photo-biohydrogen production potential of *Rhodobacter capsulatus*-PK from wheat straw Biotechnology for Biofuels, 6:144.

[54] Kars, G. and Ceylan, A. 2013. Biohydrogen and 5-aminolevulinic acid production from waste barley by *Rhodobacter sphaeroides* OU 001 in a biorefinery concept. Int J Hydrog Energy, 38:5573–9.

[55] Kaplan, I.K.; Kargi, F.; Oztekin, R. and Argun, H. 2009. Bio-hydrogen production from acid hydrolyzed wheat starch by photo-fermentation using different *Rhodobacter sp*. Int J Hydrog Energy, 34:2201–7.

[56] DHRUBAJYOTI NATH; AJAY KUMAR MANHAR; KULDEEP GUPTA; DEVA BRATT SAIKIA; SHYAMAL KUMAR DAS And MANABENDRA MANDAL. 2015. Photosynthesized iron nanoparticles: effects on fermentative hydrogen production by *Enterobacter cloacae*DH-89 Bull. Mater, Sci., Vol. 38, No. 6, pp. 1533–1538.

[57] Han, H.; Cui, M.; Wei, L.; Yang, H. and Shen J. 2011. Enhancement effect of hematite nanoparticles on fermentative hydrogen production. Bioresour Technol, 102:7903-9.

[58] Taherdanak, M.; Zilouei, H. and Karimi, K. 2015. Investigating the effects of iron and nickel nanoparticles on dark hydrogen fermentation from starch using central composite design. Int Jour Hydrogen Energy, 40:12956-63.

[59] Karadag, D. and Puhakka, J.A. 2010. Enhancement of anaerobic hydrogen production by iron and nickel. Int J Hydrogen Energy, 35(16):8554 -60.

[60] Nasr Mahmoud; Tawfik Ahmed; Ookawara Shinichi and Suzuki Masaaki. 2013. Hydrogen production from starch wastewater using anaerobic sludge immobilized on maghemite nanoparticle. In: Inter. wat. tech. conference,IWTC17.

[61] Mullai, P. ; Yogeswari, M.K. and Sridevi, K. 2013. Optimisation and enhancement of biohydrogen production using nickel nanoparticles – A novel approach Bioresource Technology, 141 212–219.

تأثير تحسين مركبات أكسيد الحديد النانوية على إنتاج الهيدروجين الحيوي التجريبي بواسطة بكتيريا التمثيل الضوئى الارجوانية اللاكبريتية

تناولت هذه الدراسه مقارنه تاثير تركزات جزيئات النانو لاكسيد الحديد على انزيمى النيتروجينيز والهيدروجينيز وكذلك انتاج الهيدروجين بواسطة ثلاثة عزلات من البكتيريا الضوئية الارجوائية اللاكبريتية وهم *Rhodobacter sphaeroides* (MG588088), *Rhodopseudomonas parapalustris* (MH094546), *Rhodopseudomonas sp.* TUT (MG813240) الذى تم تعريفهم عن طريق 16S rRNA .

تم دراسة خصائص جزيئات النانو باستخدام الميكروسكوب الالكترونى النافذ وكذالك الاسبكتروفوتوميتر واشعة اكس وجميعها اثبتت ان حجم الجزيئات وشكلها يتبع اكسيد الحديد كما اثبتت الدراسة ان تركيزات النانو المستخدمة فى المدى من ٥٠ الى ٢٥٠ ملى جرام فى اللتر ادت الى زيادة انتاج الهيدروجين لكن ١٥٠ كان افضل تركيز حيث اعطى 1.04 ,1.7 ,2.2 مول هيدروجين لكل مول جلوكوز فى حاله استخدام جزيئات النانو المستخرجه من مستخلص اوراق البرتقال و 4, 1.4 ,1.34مول هيدروجين لكل مول جلوكوز فى حاله استخدام جزيئات النانو المستخرجه من مستخلص اوراق الشاى للثلاث عزلات *Rhodobacter sphaeroides*, *Rhodopseudomonas parapalustris* *Rhodopseudomonas sp.* TUT على الترتيب كذالك اثبتت الدراسة ان جزيئات النانو المستخرجة من مستخلص نبات الشاى اعطت افضل نتائج لانتاج الهيدروجين للثلاث عزلات السابقة على الترتيب.